

Effect of Water Vapor on the Oxidation Behavior of the Eutectic High-Temperature Alloy Mo-20Si-52.8Ti

Matthias Weber,* Bronislava Gorr, Hans-Jürgen Christ, Susanne Obert, Alexander Kauffmann, and Martin Heilmaier

Herein, the effect of water vapor on the oxidation resistance of the alloy Mo-20Si-52.8Ti (at%) is investigated. The alloy is oxidized in dry, wet, as well as in situ changing atmospheres at 1100 °C. The oxidation kinetics changes from nearly parabolic to linear if water vapor is present in oxidizing atmosphere. Under all conditions, the oxide scales consist of an outer TiO₂ and a TiO₂-SiO₂ duplex layer underneath. In wet atmosphere, the thicknesses of the two regions substantially increase indicating a severe ingress of water vapor. The inferior oxidation resistance in wet environment is primarily rationalized by the fast diffusion of H₂O through SiO₂.

1. Introduction

Mo-silicide multiphase alloys are regarded as promising candidates for high-temperature structural applications such as gas turbines.^[1,2] These materials exhibit high solidus temperatures, excellent phase stability, and creep resistance.^[3] However, poor oxidation resistance is a well-known shortcoming that restricts their industrial application so far.^[4,5] Recently, outstanding oxidation resistance in air was detected for some multiphase Mo-Si-Ti alloys at 1100 and 1200 °C.^[6,7] Surprisingly, the ubiquitous pesting phenomenon at 800 °C could be reliably suppressed.^[8-10] The oxidation protectiveness of these novel alloys could be achieved by carefully controlling the chemical composition and microstructure of the alloys. At Ti contents of 43 at% and above, absence of catastrophic oxidation at 800 °C is observed even though TiO₂ is the major phase within the duplex scale.^[7]

Water vapor is one of a major component in combustion environments. The products of combustion contain ≈10% of water

vapor independent of fuel-to-air ratio.^[11,12]

It is well-known that some oxides which exhibit excellent oxidation resistance in dry air, e.g., Cr₂O₃, lose their protectiveness when H₂O is present in the oxidizing atmosphere.^[13,14] Studies on the oxidation resistance of Mo-Si-based alloys in moist air are rather limited. Hansson et al. found that the oxidation rate of MoSi₂ increases if an atmosphere with p(H₂O) = 0.1 atm is used.^[15] Moreover, an increased mass loss was recorded for MoSi₂ under wet conditions. Meschter analyzed the oxidation behavior of MoSi₂ in dry air, wet air, and

pure oxygen between 400 and 600 °C.^[16] He found that water retards the transition from nonselective to selective oxidation of Si to form a protective SiO₂ layer.^[16] Wood et al. also observed a higher mass gain of MoSi₂ in water vapor than in air in the temperature interval from 980 K (707 °C) to 1084 K (811 °C).^[17] For the first time, the effect of water vapor on the oxidation behavior of multiphase Mo-Si-B alloys was studied by Mandal et al.^[18] Although the initial mass loss due to the evaporation of MoO₃ was approximately independent on the moisture content of the atmosphere, accelerated growth of the glassy scale as well as the MoO₂ layer underneath was identified. Yet, an oxidation mechanism was not proposed in ref. [18]. To the best of our knowledge, no studies have been published on the effect of water vapor on the oxidation behavior of ternary Mo-Si-Ti alloys so far.

The aim of this work is, therefore, to gain first information about the influence of water vapor on the oxidation behavior of Ti-containing Mo-Si alloys. In this study, the oxidation behavior of a eutectic alloy with composition Mo-20Si-52.8Ti (in at%) in dry and wet atmospheres at 1100 °C is investigated. Particular attention is given onto the effect of water vapor on the formation and the growth of the oxide scales, especially of TiO₂ which forms as an outer layer and is essential in constituting the SiO₂-TiO₂ duplex scale.


2. Results and Discussion

The eutectic alloy Mo-20Si-52.8Ti consists of two phases, a bright body-centered cubic (bcc) solid solution (Mo₃Si₃Ti) and a (Ti,Mo)₅Si₃ phase (Strukturbericht D8₈), which appears dark in the backscatter electron (BSE) mode (see **Figure 1**). Both phases are presented in a nearly equal ratio. The fully lamellar eutectic alloy reveals areas of very fine as well as relatively coarse microstructures. The microstructure of the alloy Mo-20Si-52.8Ti

M. Weber, Dr. B. Gorr, Prof. H.-J. Christ
Institut für Werkstofftechnik
Universität Siegen

Paul Bonatz Str. 9-11, Siegen 57068, Germany
E-mail: matthias.weber@uni-siegen.de

S. Obert, Dr. A. Kauffmann, Prof. M. Heilmaier
Institut für Angewandte Materialien
Karlsruhe Institut für Technologie (KIT)
Engelbert-Arnold-Str. 4, Karlsruhe 76131, Germany

 The ORCID identification number(s) for the author(s) of this article can be found under <https://doi.org/10.1002/adem.202000219>.

© 2020 The Authors. Published by WILEY-VCH Verlag GmbH & Co. KGaA, Weinheim. This is an open access article under the terms of the Creative Commons Attribution License, which permits use, distribution and reproduction in any medium, provided the original work is properly cited.

DOI: 10.1002/adem.202000219

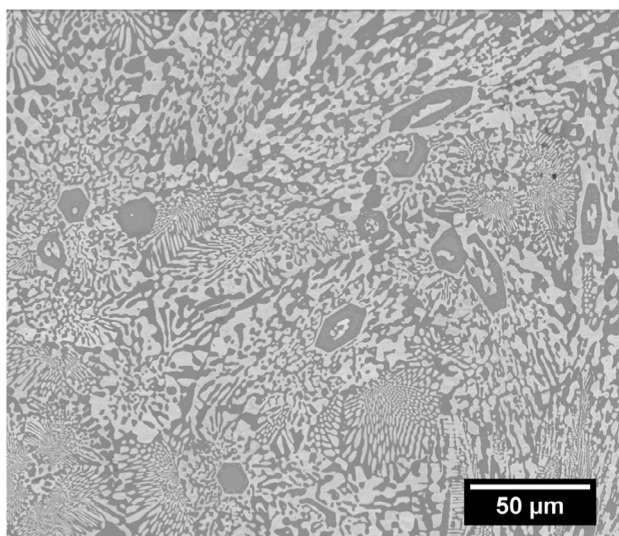


Figure 1. BSE image of the alloy Mo-20Si-52.8Ti.

Table 1. Oxidation tests, oxidizing atmosphere, and test duration.

Oxidation test/sample	Atmosphere	Total oxidation time [h]
1	50 h dry	50
2	50 h wet	50
3	50 h dry + 50 h wet	100
4	50 h dry + 100 h wet	150
5	50 h wet + 50 h dry	100
6	50 h dry + 50 h wet + 50 h dry	150

was described in detail in refs. [6,7]. **Table 1** summarizes the experiments performed in this work, the corresponding atmospheres, and test durations. **Figure 2** shows the oxidation kinetics of the alloy Mo-20Si-52.8Ti recorded during continuous oxidation tests at 1100 °C. Oxidation experiments given in Table 1 were performed several times (except of tests 4 and 5) to prove reproducibility. Comparing the oxidation curves of the samples oxidized in dry (sample 1, black curve in Figure 2a) and wet

(sample 2, black curve in Figure 2b) atmosphere for 50 h, a more intense oxidation attack during oxidation in water vapor containing gas can be concluded due to a higher mass gain of the sample 2. It should be pointed out that mass loss, which is typical of B-containing Mo-silicide alloys, was detected neither in dry nor in wet surroundings.^[19] Moreover, the decelerating oxidation kinetics was detected during exposure to both single atmospheres.

Oxidation kinetics of sample 3, which represents oxidation under changing conditions, i.e., exposure to dry air for 50 h followed by 50 h in wet atmosphere, exhibits a clear accelerating character toward linear oxidation while exposure to wet surrounding. Furthermore, this trend seems to be consistent with the oxidation kinetics of sample 4 (50 h dry + 100 h wet); see the blue curve Figure 2a. In contrast, no significant change in the oxidation kinetics was observed when the test atmosphere is changed from wet to dry (sample 5), though, a lower mass gain during oxidation under dry conditions would be anticipated. The thermogravimetric signal of sample 6 (green curve in Figure 2a) represents the most sophisticated experiment in this study. The linear oxidation in the wet surrounding during the second 50 h follows the decelerating kinetics during oxidation in dry air within the first 50 h. During the last 50 h of oxidation under dry conditions, the kinetics is significantly slowed down. Interestingly, the mass gain of sample 6 during the last 50 h oxidation in dry surroundings is substantially less pronounced compared with the last 50 h under dry conditions of sample 5. Apparently, the initial atmosphere and the properties of the initially formed oxide scales crucially affect the following oxidation behavior.

In conclusion, the thermogravimetric data presented in Figure 2 indicate that 1) water vapor changes the properties of the oxide scale unfavorably leading to accelerated kinetics and 2) the oxide scale initially formed in a particular atmosphere determines the later oxidation behavior.

The microstructural analyses of the oxide scales formed on the samples 1–6 should provide additional information to allow proper interpretation of the thermogravimetric results. **Figure 3a,b** show the cross-sectional micrographs and the results of the energy-dispersive X-ray spectroscopy (EDX) analyses of the samples oxidized at 1100 °C in dry and wet atmospheres, respectively. Clearly, the oxide scale formed in wet surroundings is substantially thicker compared with that formed under dry conditions.

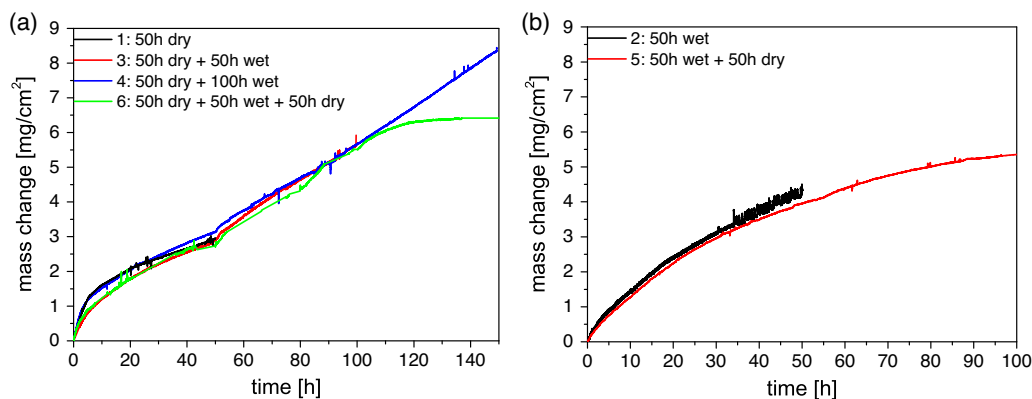


Figure 2. Oxidation kinetics of the alloy Mo-20Si-52.8Ti at 1100 °C in different atmospheres; a) samples 1, 3, 4, 6 and b) samples 2 and 5; for the sample identification see Table 1.

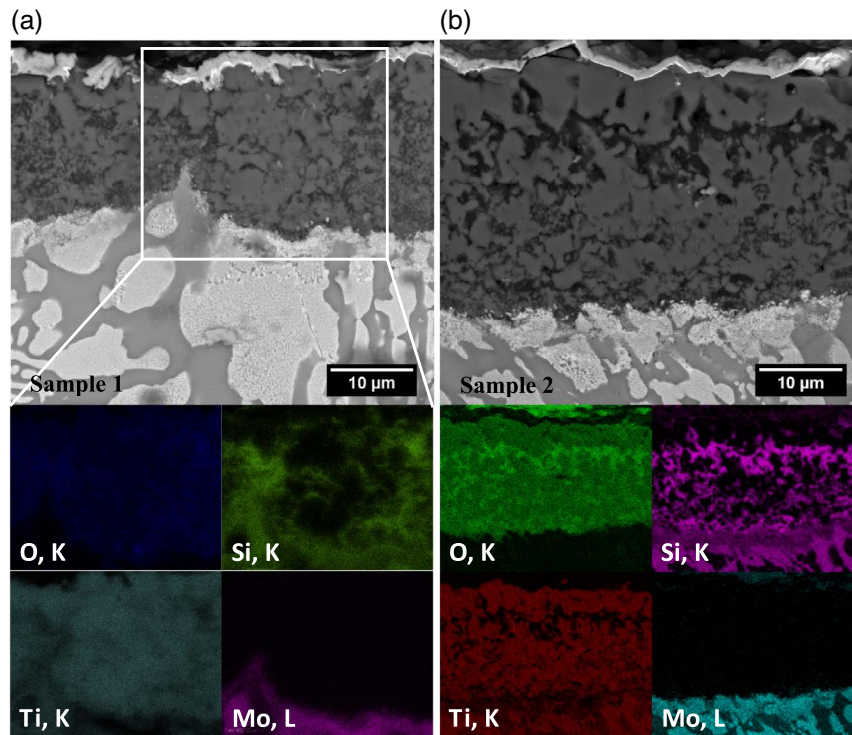


Figure 3. Cross-section (BSE mode) and the EDX analyses of the alloy Mo-20Si-52.8Ti oxidized at 1100 °C for 50 h in a) dry atmosphere (sample 1) and b) water vapor containing atmosphere (sample 2).

This finding confirms the thermogravimetric data presented in Figure 2 (compare mass gains of samples 1 and 2). The crystal structure and constitution of the oxide scales were determined by means of X-ray diffraction (XRD) and EDX. The results of the XRD measurements (Figure 4) of the sample 1 and 2 reveal the formation of TiO_2 , SiO_2 , and MoO_3 . Clearly, molybdenum oxide hydrate additionally forms during oxidation in a water vapor containing atmosphere. Both samples form a duplex layer

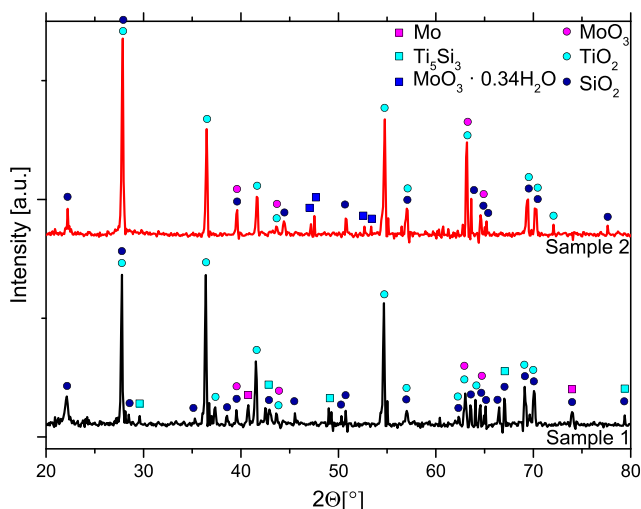


Figure 4. XRD plots of Mo-20Si-52.8Ti after 50 h oxidation at 1100 °C in dry and water vapor containing atmosphere.

consisting of TiO_2 (light gray level in Figure 3) and SiO_2 (dark gray level in Figure 3) at the substrate/oxide interface. The TiO_2 phase fraction of the sample exposed to wet atmosphere (Figure 3b) seems to be lower (53%) compared with the counterpart oxidized in dry air (65%) (Figure 3a). In addition, a more pronounced outer TiO_2 scale (Figure 3b) is observed on the sample after exposure to wet atmosphere, whereas this layer is hardly recognizable on the sample oxidized in dry surroundings.

Figure 5a–d show cross-sectional micrographs and the results of EDX analyses of the samples oxidized in in situ changing atmospheres (see samples 3–6 in Table 1). All oxide scales formed in consecutively changing atmospheres appear rather similar exhibiting the two-layered structure well-known from the tests in static atmospheres, i.e., an outer TiO_2 scale and a duplex $\text{TiO}_2/\text{SiO}_2$ scale underneath. The results of the XRD measurements (Figure 6) reveal that the substrate peaks disappear indicating the formation of rather thick oxide layers. Moreover, the corresponding peaks of the molybdenum oxide hydrate were also not observed. To reveal possible subtle distinctions between the oxide scales grown in different atmospheres, a quantitative analysis of the oxide scales formed on the samples 1–6 was conducted. The following characteristics of the oxide scales were determined for the individual samples: 1) the total thickness of the oxide scale and 2) the thickness of the outer TiO_2 layer.

Figure 7 shows the evaluated thicknesses of the oxide scales grown on the samples 1–6. As expected, the lowest (total) oxide thickness was measured for sample 1 (50 h dry), whereas the highest value was found for sample 4 (50 h dry + 100 h wet) which was exposed to the wet atmosphere the longest. The total

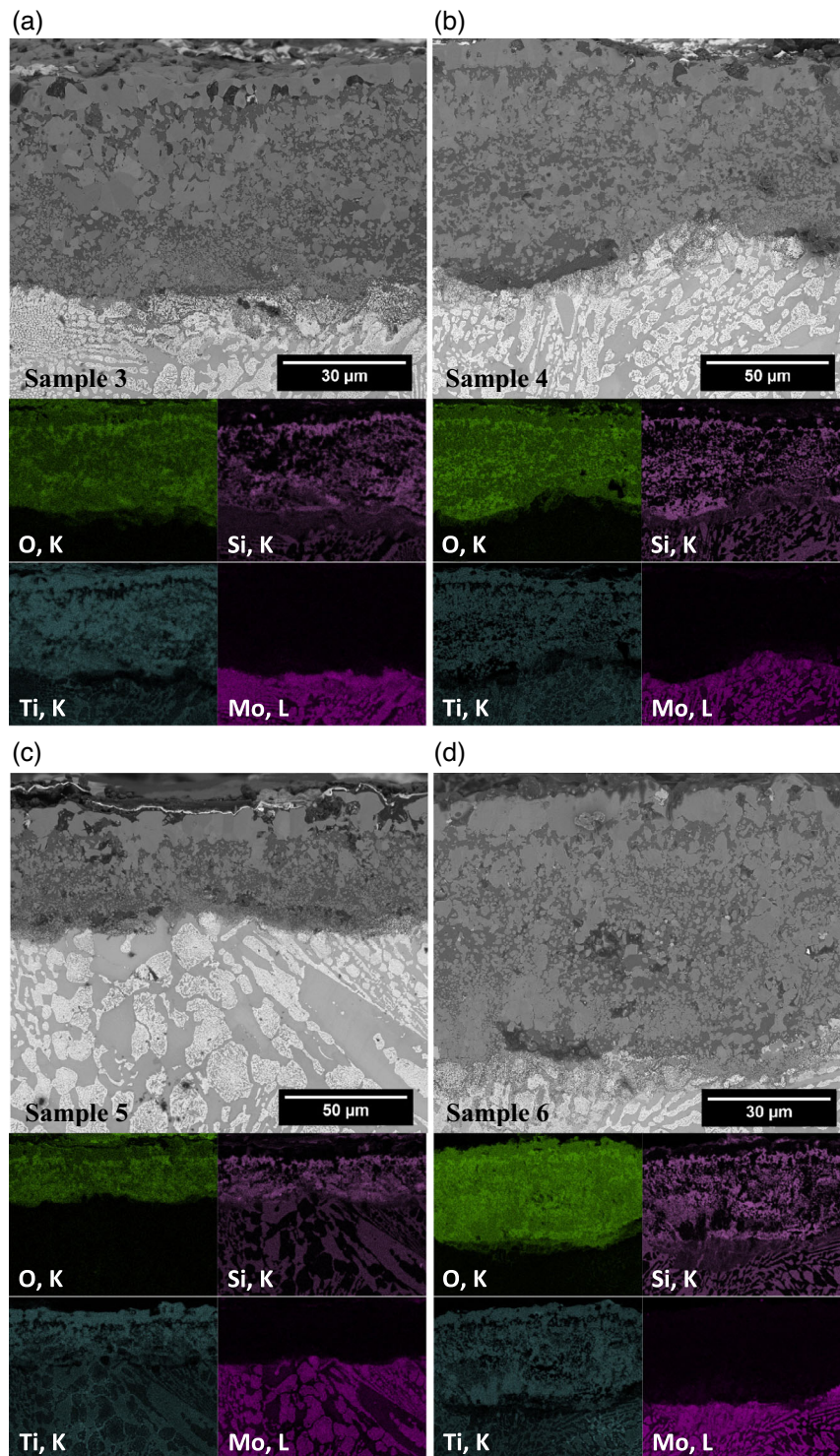


Figure 5. Oxide scales (in BSE mode and corresponding EDX analyses) formed on the alloy Mo-20Si-52.8Ti during oxidation experiments with in situ changing atmospheres at 1100 °C; a) 50 h dry + 50 h wet (sample 3), b) 50 h dry + 100 h wet (4), c) 50 h wet + 50 h dry (5), and d) 50 h dry + 50 h wet + 50 h dry (6).

scale thicknesses are in good agreement with the thermogravimetric weight gains shown in Figure 2. Comparing solely the TiO₂ outer scale thicknesses of the sample 1 (50 h dry) and

sample 2 (50 h wet), it was found that the titania layer grows faster in wet than in dry surroundings suggesting faster diffusion if H₂O is present in the oxidizing atmosphere.

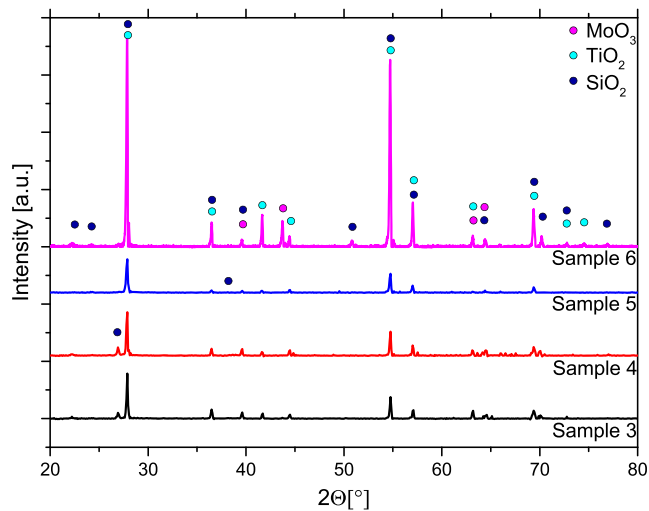


Figure 6. XRD plots of Mo-20Si-52.8Ti after oxidation in in situ changing atmospheres at 1100 °C.

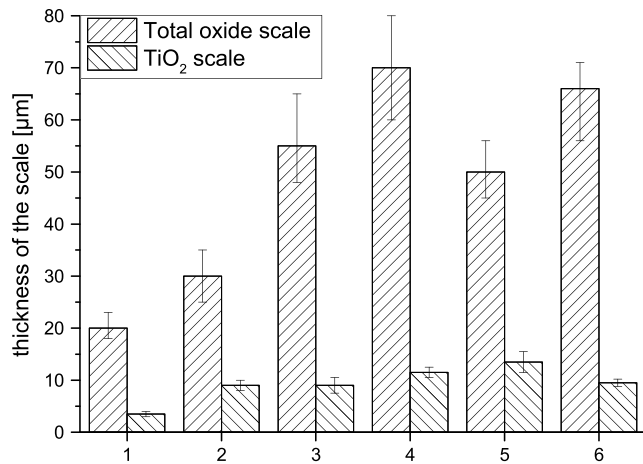


Figure 7. Thicknesses of the total oxide scale and the outer TiO₂ layer formed on Mo-20Si-52.8Ti during oxidation experiments at 1100 °C.

A quantitative comparison of the data shown in Figure 7 is difficult because of different oxidation durations and varying oxidizing atmospheres. To compare the scales formed during oxidation in in situ changing atmospheres, the contributions to the overall oxide scale thickness and the outer TiO₂ oxide scale of individual periods in a particular atmosphere are shown in Figure 8 and 9, respectively. For the sake of completeness, the thicknesses of oxide scales grown in the first 50 h are also included in Figure 8. Note that these numbers represent absolute values of the oxide thicknesses in contrast to the differences for the second 50 h and the third 50 h. Nevertheless, these data can be considered for the analysis in Figure 8 as they give reference to the state prior to oxidation. The results summarized in Figure 8 unequivocally show that the oxide scales grow substantially quicker in wet than in dry surroundings on Mo-20Si-52.8Ti under all testing conditions. This trend is confirmed for the first 50 h as well as for the second and the third 50 h of oxidation.

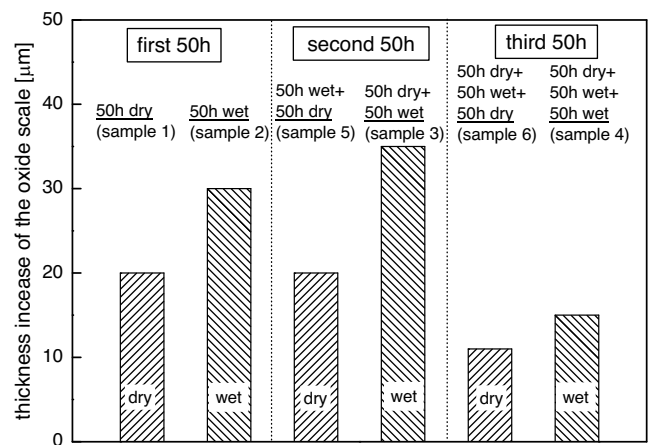


Figure 8. Thickness increase of the (total) scale formed on the alloy Mo-20Si-52.8Ti during oxidation experiments with in situ changing atmospheres at 1100 °C.

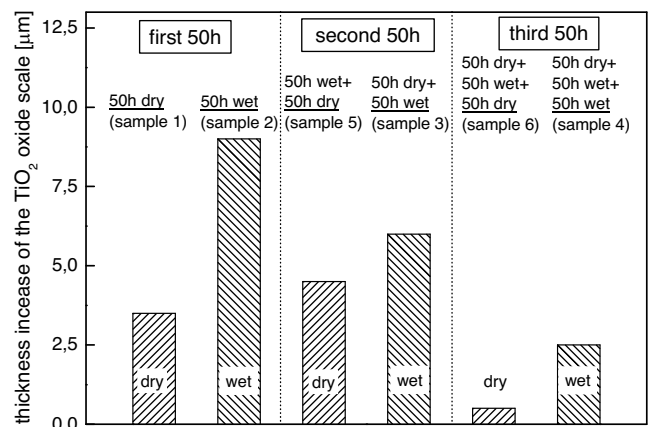


Figure 9. Thickness evolution of the outer TiO₂ layer formed on Mo-20Si-52.8Ti during oxidation experiments with in situ changing atmospheres at 1100 °C.

Melsheimer et al. investigated the oxidation performance of TiSi₂ which forms an oxide scale similar to that found on our alloy.^[20] To understand the oxidation mechanism, a Pt marker experiment was conducted revealing that external growth of the TiO₂ layer accounts for the Ti outward diffusion, whereas the SiO₂–TiO₂ duplex layer underneath grows as a result of the O inward diffusion.^[20] A similar conclusion was drawn by Burk et al. who investigated the oxidation behavior of monolithic (Mo,Ti)₅Si₃ in dry air.^[21] Therefore, it is reasonable to assume that the same mechanism also holds true for Mo-20Si-52.8Ti. The main intention of the present study is to explore whether the aforementioned oxidation mechanism is affected by water vapor. As the oxide scale consists of two types of oxides, namely TiO₂ and SiO₂, the effect of water vapor on both oxides should be studied separately.

Results of multiple experimental studies provide sound evidence that the oxidation rate of silica scale-forming alloys increases if water vapor is added to oxidizing surroundings.^[16–18] The diffusion of water in silica in the temperature range from

600 to 1200 °C was studied by Roberts and co-workers.^[22,23] It was concluded that molecular water diffuses into glass and reacts with the silicon/oxygen network of the glass, leading to the formation of SiOH groups according to Equation (1). Tracer experiments were performed using water labeled with deuterium, tritium, and the stable isotope O¹⁸. It was found that SiOH groups are relatively immobile, however, the defects and strains in silica can increase the rate of diffusion of OH groups.^[24] Moreover, according to Doremus, OH groups can recombine to form water molecules in silica.^[25]



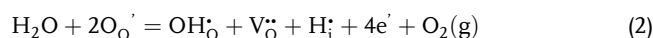
Furthermore, some theoretical studies dealt with the diffusion and reaction mechanism describing the diffusion of water into silica glass.^[26,27] Wolters, for example, who analyzed interactions of O₂-H₂O mixtures with silica, proposed that solubility of water proceeds in two steps at temperatures up to 1100 °C: 1) the slow formation of SiOH groups (the mobility of which can be neglected) and 2) the fast hydrolyzation and the formation of H₃O⁺ and SiOH⁻.^[27] Finally, it was shown that water migrates through silica by H₃O⁺ and OH⁻.^[27] It was, thus, concluded that water may play a significant role in the oxidation rate even at a dilute level. As the effective diffusion coefficient of water is two orders of magnitude higher than that of oxygen, water plays an equal role in the oxidation process when the partial pressure is only 1%, i.e., $p_{\text{H}_2\text{O}} = 0.01p_{\text{O}_2}$.^[27] It was further assumed that oxygen and water species do not diffuse independently. This assumption was confirmed by Irene and Ghez who investigated the parallel and independent transport of water and oxygen.^[28] It was observed that the parabolic rate constant increases abruptly with small additions of H₂O to O₂, whereas the linear rate constant enhances gradually over the range of added H₂O. They finally concluded that water acts both, as an additional source of oxidant and as an accelerator for the oxidation process involving oxygen. The influence of water was explained by loosening the silica network allowing the oxygen to move faster.^[28] The experimental results presented in this study lead to a suggestion that the mechanism proposed by Irene and Ghez seems to hold true for Mo-20Si-52.8Ti investigated in this work.

Figure 9 shows the increase in thickness of the outer TiO₂ layer depending on the oxidation time and atmosphere. For the data in Figure 9, the same approach as for the thickness of the total oxide scale was applied. The TiO₂ layer seems to grow notably faster in wet than in dry atmospheres. There are only few studies reported on the interaction of TiO₂ with water vapor. Shimada et al. investigated the oxidation behavior of TiC ceramics in dry and wet atmospheres including oxidation in ¹⁶O₂/¹⁸O gas mixtures at 900–1200 °C.^[29] The formation of H₂/H was detected at the interface indicating the reaction of TiC with H₂O, resulting in significantly higher oxidation rates in wet than in dry gases. Moreover, it was found that the presence of water vapor promotes the grain growth of TiO₂, leading to a sintering-like effect and, therefore, more dominant volume diffusion.

The defect structure of TiO₂ is rather complex as conflicting statements are found in literature. Hurlen and Tannhauser suggested that interstitial Ti ions are the most probable defect type in TiO₂, whereas Kofstad proposed that TiO₂ predominantly

contains double charged O vacancies.^[30–33] Clearly, the defect structure of TiO₂ becomes even more complex if growing in water vapor containing atmosphere. Bredow and Jug investigated the water adsorption at TiO₂ surfaces and concluded that the dissociative adsorption, which primarily takes place at defect sites, e.g., at O vacancies, is more stable than the molecular adsorption.^[34]

It is well-known that rutile is an n-type semiconductor.^[33] As a possible interaction between H₂O and TiO₂, Equation (2) can be proposed. According to it, two O²⁻ ions leave their normal lattice sites, are discharged putting four electrons in the conduction band and finally released to the atmosphere as an oxygen molecule. Although one anion site is occupied by OH⁻, an anion vacancy is built on the second anion lattice site. Hydrogen from the H₂O molecule is incorporated in the TiO₂ lattice as an interstitial proton H⁺. The crucial result of the proposed interaction between H₂O and TiO₂ is the increase in the oxygen vacancy concentration. Such an effect would accelerate the oxygen inward diffusion and increase the oxide growth rate of TiO₂. The proposed mechanism is strongly supported by experimental results demonstrated in Figure 9, which show that TiO₂ grows substantially faster in wet environments than in dry atmosphere. Liu and Narit also observed the accelerated formation of TiO₂ on γ-TiAl at 800 °C if water is added to the oxidizing atmosphere.^[35] Unfortunately, this experimental finding was not elucidated.



Another important issue is the formation of hydroxides of both, Si and Ti. However, the oxidation temperature of 1100 °C is too low to trigger the notable evaporation of hydroxides. The formation and volatilization of Si(OH)₄ becomes critical at temperature above 1200 °C.^[36] Significant mass loss of TiO₂ attributed to the formation of Ti(OH)₄ was reported by Ueno et al. at a significantly higher temperature of 1500 °C.^[37] Meschter et al. pointed out in their review that further investigations of TiO₂ volatilization in water-vapor-rich atmospheres are required because of conflicting results reported in literature.^[36]

3. Conclusion

In this study, the oxidation behavior of a two-phase, eutectic Mo-20Si-52.8Ti alloy was investigated in dry and wet atmospheres at 1100 °C. The experimental findings can be summarized as follows: 1) During exposure to dry atmosphere, very moderate values of mass gain were detected. Accelerated linear kinetic was observed during oxidation in wet atmosphere indicating more severe oxygen and presumably also H₃O⁺ and OH⁻ ingress. The experiments with in situ changing atmospheres additionally reveal a sensitivity of the oxidation kinetics upon the oxidation environment; 2) Both oxide scales, the outer TiO₂ layer as well as the duplex scale SiO₂-TiO₂ underneath, grow substantially faster in wet than in dry surroundings; 3) From the present experiments it is concluded that the defect concentration in TiO₂ unfavorably changes if H₂O is present in the atmosphere, resulting in thicker TiO₂ scales.

Future studies will be directed to increasing oxidation temperatures and varying water vapor pressures in the testing

atmosphere to make the currently subtle distinctions between the oxide scales formed in dry and wet gases more noticeable. It will be of particular interest to study whether the outer TiO₂ layer prevents the evaporation of Si hydroxide(s). The experimental results presented in this work clearly show that that water vapor accelerates oxidation processes and an appropriate environmental barrier coating (EBC) system is required for Mo–Si–Ti alloys if exposed to wet surroundings. The point is addressed in the companion article by Anton et al. of the current issue.^[38]

4. Experimental Section

The alloy Mo-20Si-52.8Ti (at%) was manufactured from elemental bulk materials by arc melting (arc melter AM 0.5 of Edmund Bühler GmbH) in an Ar atmosphere. The purities of the raw elements Si, Mo, and Ti were 99.99%, 99.95%, and 99.8%, respectively. The prepared buttons were turned over and remelted at least five times in a water-cooled Cu mold to homogenize the alloy. The ingots were then cut to 5 × 7.5 × 2 mm³ dimension by electrical discharge machining (EDM). The EDM surfaces were ground down to SiC grit P1200. Just before high temperature exposure, the samples were cleaned in ethanol in an ultrasonic bath. Oxidation tests were performed in a thermogravimetric Rubotherm system under isothermal conditions at 1100 °C in dry laboratory air (designated as dry) and wet atmosphere (Ar–10%N₂–20%O₂–10%H₂O gas mixture, designated as wet). To establish the required wet atmosphere, the thermogravimetric device was floated with water vapor containing mixture for 2 h prior to sample exposure. The gas flow during the oxidation experiments was set to a rate of 6 L h⁻¹. Within the same experimental setup, some samples were exposed to changes alternating between dry and wet atmospheres with a cycle time of 50 h.

The crystal structures of the oxides formed on the surface were analyzed using XRD. The XRD measurements were performed with an X'Pert Pro MPD in Bragg–Brentano geometry with Cu–Kα radiation. After the oxidation tests, the samples were coated with a conductive Au layer and then galvanically Cu-plated. Afterward, the samples were wrapped in Al foil, embedded in resin and ground to SiC grit P4000, and vibratory polished with a 0.05 μm silica suspension. The oxide scale morphology was analyzed by means of a focused ion beam/scanning electron microscope (FIB/SEM) dual beam system (FEI Helios Nanolab 600). It was equipped with a BSE detector, an EDX detector, and an electron backscatter diffraction system (EBSD). The mean oxide layer thicknesses were determined by analyzing BSE cross-sectional images using the image-processing software ImageJ.

Acknowledgements

This work was conducted under the financial support of Deutsche Forschungsgemeinschaft (DFG) within the framework of grant no. GO2283/3-1 and HE 1872/33-1, which is gratefully acknowledged. For the scientific and technical support at the University of Siegen, the authors thank W. Kramer. Part of this work was performed at the Micro- and Nanoanalytics Facility (MNAF) of the University of Siegen.

Conflict of Interest

The authors declare no conflict of interest.

Keywords

hydroxides, Mo–Si–Ti-based alloys, water vapor

Received: February 21, 2020

Revised: April 22, 2020

Published online:

- [1] J. H. Perepezko, *Science* **2009**, 326, 1068.
- [2] S. Y. Kamata, D. Kanekon, Y. Lu, N. Sekido, K. Maruyama, G. Eggeler, K. Yoshimi, *Sci. Rep.* **2018**, 8, 10487.
- [3] D. M. Berczik, *US Patent No. 5,693,156*, **1997**.
- [4] M. K. Meyer, A. J. Thom, M. Akinc, *Intermetallics* **1999**, 7, 153.
- [5] A. Gulec, X. Yu, M. Taylor, A. Yoon, J.-M. Zuo, J. Perepezko, L. Marks, *Corrosion* **2018**, 74, 288.
- [6] D. Schliephake, A. Kaufmann, X. Cong, C. Gombola, M. Azim, B. Gorr, H.-J. Christ, M. Heilmaier, *Intermetallics* **2019**, 104, 133.
- [7] S. Obert, A. Kaufmann, M. Heilmaier, *Acta Mater.* **2020**, 184, 132.
- [8] H. J. Grabke, G. H. Meier, *Oxid. Met.* **1995**, 44, 147.
- [9] M. Azim, D. Schliephake, C. Hochmuth, B. Gorr, H.-J. Christ, U. Glatzel, M. Heilmaier, *JOM* **2015**, 67, 2621.
- [10] R. Tewari, N. K. Sarkar, D. Harish, B. Vishwanadh, G. K. Dey, S. Banerjee, *Materials Under Extreme Conditions: Recent Trends and Future Prospects* (Eds: A. K. Tyagi, S. Banerjee), Elsevier, Amsterdam **2017**, pp. 319–320.
- [11] N. S. Jacobson, *J. Am. Ceram. Soc.* **1993**, 76, 3.
- [12] M. P. Boyce, *Advanced Industrial Gas Turbines for Power Generation* (Ed: A. D. Rao), Woodhead Publishing Limited, Cambridge **2012**, pp. 62–74.
- [13] D. J. Young, *High Temperature Oxidation and Corrosion of Metals*, Elsevier, New York **2008**, pp. 459–466.
- [14] S. K. Arifin, M. Hamid, A. N. Berahim, M. H. Ani, *IOP Conf. Ser.: Mater. Sci. Eng.* **2018**, 290, 012085.
- [15] K. Hansson, M. Halvarsson, J. Tang, R. Pompe, M. Sundberg, J.-E. Svensson, *J. Eur. Ceram. Soc.* **2004**, 24, 3559.
- [16] P. J. Meschter, *Metall. Trans. A* **1992**, 23, 1763.
- [17] E. Wood, S. S. Parker, A. T. Nelson, S. A. Maloy, *J. Am. Ceram. Soc.* **2016**, 99, 1412.
- [18] P. Mandal, A. J. Thom, M. J. Kramer, V. Behrani, M. Akinc, *Mater. Sci. Eng. A* **2004**, 371, 335.
- [19] S. Burk, B. Gorr, V. B. Trindade, H.-J. Christ, *Oxid. Met.* **2010**, 73, 163.
- [20] S. Melsheimer, M. Fietzek, V. Kolarik, A. Rahmel, M. Schütze, *Oxid. Met.* **1997**, 47, 139.
- [21] S. Burk, B. Gorr, H.-J. Christ, D. Schliephake, M. Heilmaier, C. Hochmuth, U. Glatzel, *Scr. Mater.* **2012**, 66, 223.
- [22] A. J. Moulson, J. P. Roberts, *Trans. Faraday Soc.* **1961**, 57, 1208.
- [23] I. Burn, J. P. Roberts, *Phys. Chem. Glasses* **1970**, 11, 106.
- [24] G. J. Roberts, J. P. Roberts, *Phys. Chem. Glasses* **1964**, 5, 26.
- [25] R. H. Doremus, *J. Mater. Res.* **1995**, 10, 2379.
- [26] R. H. Doremus, *J. Mater. Res.* **1995**, 10, 2379.
- [27] D. R. Wolters, *J. Electrochem. Soc.* **1980**, 127, 2072.
- [28] E. A. Irene, R. Ghez, *J. Electrochem. Soc.* **1977**, 124, 1757.
- [29] S. Shimada, T. Onuma, H. Kiyono, M. Desmaison, *J. Am. Ceram. Soc.* **2006**, 89, 1218.
- [30] T. Hurlen, *Acta Chem. Scand.* **1959**, 13, 365.
- [31] D. S. Tannhauser, *Solid State Commun.* **1963**, 1, 223.
- [32] P. Kofstad, *J. Phys. Chem. Solids* **1962**, 23, 1579.
- [33] P. Kofstad, *High Temperature Oxidation of Metals*, Wiley, New York **1966**, pp. 68–73.
- [34] T. Bredow, K. Jug, *Surf. Sci.* **1995**, 327, 398.
- [35] Z. Liu, T. Narit, *Intermetallics* **2003**, 11, 795.
- [36] P. J. Meschter, E. J. Opila, N. S. Jacobson, *Ann. Rev. Mater. Res.* **2013**, 43, 559.
- [37] S. Ueno, D. D. Jayaseelan, N. Kondo, T. Ohji, S. Kanzaki, *Mater. Trans.* **2004**, 45, 281.
- [38] R. Anton, N. Laska, U. Schulz, S. Obert, M. Heilmaier *Adv. Eng. Mater.* **2020**, <https://doi.org/10.1002/adem.202000218>.